Cent. Eur. J. Phys. • 8(2) • 2010 • 184-193
DOI: 10.2478/s11534-009-0073-1

VERSITA

Central European Journal of **Physics**

Alkali lasers for magnetic resonance imaging

Research Article

Boris V. Zhdanov*, Randall J. Knize

US Air Force Academy, Department of Physics, Laser and Optics Research Center, 2354 Fairchild Dr., Ste. 2A31,USAF Academy, CO 80840, USA

Received 9 December 2008; accepted 3 April 2009

Abstract: Spin-polarized nuclei of such gases as ^{3}He and ^{129}Xe are successfully used for magnetic resonance imaging of lungs and other organs of human body. To produce large numbers of spin-polarized nuclei required for this medical application, a high power narrowband tunable laser source is required. Diode pumped alkali lasers, developed during last several years can be an ideal source for this application. In this paper we present our latest achievements in diode pumped alkali lasers development. We describe optically pumped Cs laser tunable in the range of 14 GHz and operating in single transverse mode with a linewidth less than 3 MHz. We also present continuous wave diode pumped Rb and Cs lasers with output power 17 W and 20 W.

PACS (2008): 42.55.-f; 42.55.Lt; 42.55.Xi; 42.60.By; 42.62.Be

Keywords: MRI imaging • spin polarized nuclei • alkali lasers

1. Introduction

Magnetic Resonance Imaging (MRI) (or Nuclear magnetic resonance imaging (NMRI)) is a medical imaging technique most commonly used in Radiology to visualize the structure and function of the body. It provides detailed images of the body in any plane with a better contrast than Computed Tomography does. MRI is used to image every part of the body, but is particularly useful in neurological conditions, disorders of the muscles and joints, for evaluating tumors and showing abnormalities in the heart and blood vessels. Unlike Computed Tomography, scanning MRI uses no ionizing radiation and is generally a very safe procedure.

*E-mail: boris.zhdanov.ctr@usafa.edu

MRI usually uses proton nuclear magnetic resonance, aligning nuclear magnetization of hydrogen atoms in a magnetic field (so called, spin polarization), and then alter this alignment by a radiofrequency field to produce a rotating magnetic field detectable by the scanner. This signal is used to build up information to reconstruct an image of the body.

Essentially, MRI provides a map of distribution of hydrogen atoms (protons) density in the human body. The success of MRI depends on concentration of hydrogen atoms in tissue and it is highest in water and fat. That means, that there can be problems with imaging organs with low water density, for example gas spaces in lungs. A 1.5 T magnetic field can provide a concentration of spin polarized atoms about 10^{-6} of total proton density [1], which is enough for imaging water in tissue. But, the density of water vapor is 10^{-4} of the density of water in tissue and this makes problematic the use of proton NMRI for

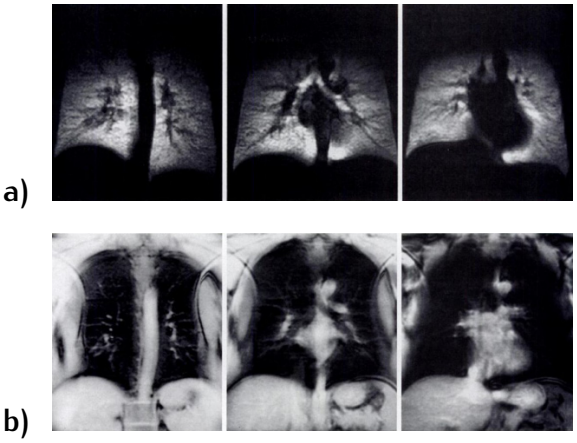

Figure 1. MRI of lungs using spin polarized He-3 (a) and usual H-1 (b).

imaging of lungs and gas movement in the body.

One solution of this problem is the use of specially prepared "spin polarized" noble gases [2], which can be inhaled by humans without any harm and show gas spaces and gas movements in the human body. Experiments on spin polarization of He-3 and Xe-129 by collisions with optically pumped alkali atoms showed that spin polarization values can be higher than 50% and this gives 10^5 – 10^6 NMR signal enhancement compared to H-1. The latter makes possible imaging of the gas spaces filled with these noble gases. Fig. 1 obtained by MacFall et. al [1] demonstrates difference between MRI images of lungs obtained with spin polarized He-3 (a) and the corresponding images obtained using usual H-1 (b). It is well seen, that using spin polarized He-3 provides images of gas spaces in lungs that cannot be obtained by usual MRI with H-1. The essential feature of this method is the use of a spin polarized noble gas, which can be produced by spin-exchange optical pumping.

The process of the spin exchange optical pumping is described in details in many publications (see, for example, [3]). In general, it consists of two stages. The first stage is the optical pumping of an alkali vapor by a circularly polarized light resonant to the $D1$ transition of the alkali atom. As a result of this pumping, the polarization of electronic spin of the alkali atoms is produced. Then, the spin polarized alkali atoms collide with noble gas atoms and transfer the spin polarization to the noble gas atoms. After separating the inert noble gas from the alkali vapors, it can be inhaled by humans and used for MRI imaging.

The essential part of the spin exchange optical pumping procedure is an appropriate laser light source, which has several requirements. First, its operation wavelength should match the $D1$ line of alkali atom (e.g. 795 nm for Rb or 895 nm for Cs). Second, the linewidth of this laser must be narrower than the alkali absorption band (10 GHz at 1 atm pressure of gas). Then, the output power of this source must be high enough (at least several tens of Watts) to effectively produce spin polarized noble gas. And, at last, such laser must have high enough wall plug efficiency, more or less simple design, and must be dependable and commercially available.

There are several lasers, which were used in the experiments on spin exchange optical pumping. They are Titanium-Sapphire lasers, Dye lasers and Diode lasers. None of these lasers satisfies all the listed above requirements. They are either very complicated, expensive, low power and not efficient (Ti:Sa and Dye lasers) or too broadband with poor beam quality (diode lasers). The alternative light source is a new type of lasers, namely, diode pumped alkali vapor laser (DPAL) [4], which is under intensive development during the last several years [5–10].

DPAL can be an efficient laser for the spin exchange optical pumping application. It has very narrow linewidth (less than 3 GHz) and it is tunable enough for fine tuning to the alkali atoms $D1$ line. Its operating wavelength matches the absorption $D1$ line of the corresponding alkali atom, because it lases on the same atomic transition. It is very efficient (more than 80% slope efficiency demonstrated) and has high output power: Rb laser with 17 W output [11] and Cs laser with 48 W output [9] have been demonstrated. And, if necessary, the output power of these lasers can be scaled to higher value. In addition, these lasers have simple design, high wall plug efficiency and can be produced commercially for many other applications. The goal of this paper is to review the main achievements in the field of the DPAL research and development.

2. Alkali lasers – optically pumped gas lasers

The first optically pumped alkali (potassium) vapor laser was proposed by Schawlow and Townes (they called it an "optical maser") in 1958 [12], even before the first laser was demonstrated by Maiman in 1961 [13]. Laser gain in an optically pumped Cs vapor was measured in 1961 [14], and the first laser action in alkali atoms (Cs) at 7.18 μm was observed in 1962 using a helium lamp as a pump [15]. The lasing efficiency in these experiments was very low, and the output power did not exceed 50 μW. After these initial experiments with alkali atoms, there were various demonstrations of stimulated emission, gain and amplified spontaneous emission in alkali vapors in the next 40 years. Numerous theoretical and experimental studies of

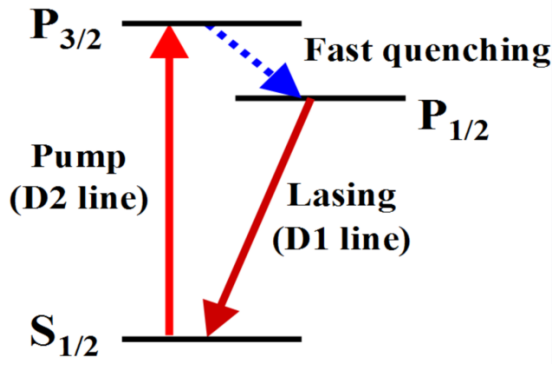

Figure 2. Alkali Lasers Energy Level Diagram.

energy transfer, energy levels mixing and a 3-level lasing in alkalis were performed during that time. But the real interest to these lasers appeared only in the last several years, when efficient and high power diode laser pump sources were developed.

All optically pumped alkali lasers operate using three-level pump scheme (see Fig. 2) described by Konefal [16]. Pump radiation from an external laser source excites the alkali atom $D2$ line and buffer gas (usually, ethane at a pressure of 50 - 500 torr) provides effective collisional transfer from the $P_{3/2}$ state to the $P_{1/2}$ state. Lasing occurs on the $P_{1/2} \rightarrow S_{1/2}$ transition ($D1$ line). The first demonstrations of an efficient optically pumped alkali lasers (Cs and Rb) were performed by Krupke et al. in 2003-2004 [4, 17]. They used a Ti:Sapphire laser as a pump source and demonstrated a slope efficiency of more than 5%. The efficiencies reported in these experiments were "relative to the absorbed power" and the real efficiencies (relative to the pump power) were several times lower because the linewidth of the pump laser used in these experiments (30 – 50 GHz) didn't match the absorption linewidth of the alkali vapors (about 10 GHz). Later, using a narrowband Ti:Sapphire laser pump source, we have demonstrated Cs laser with 81% slope and 63% overall optical efficiency [7], what is still the best result for alkali lasers.

3. Diode laser pumping for alkali lasers

Experiments on Alkali lasers performed with a Ti:Sapphire laser pump had demonstrated high efficiency of these lasers, but couldn't demonstrate high output power, because of limited power of the pump sources. Using efficient high power diode lasers for pumping of alkali vapors promises a significant increase not only in the laser output power, but in total wall plug efficiency as well. That is why experiments with diode pumping of alkali lasers were always of great interest and importance.

The first alkali (Cs) laser operating with a diode laser pump was demonstrated in 2005 [18]. We used a narrowband diode laser operating at 852 nm (SDL-8630, linewidth is less than 1 MHz) to longitudinally pump a 5 cm long Cs vapor cell. A maximum slope efficiency of 41% and a maximum output power of 130 mW were obtained in this experiment. To increase the output power, a more powerful diode laser, laser diode arrays (LDAs) or stacks of arrays must be used.

Commercially available LDAs, operating in a CW mode, can generate hundreds of watts of laser power in near-IR with a typical linewidth of several nm (or about 1 THz). The main problem in using of the LDAs for alkali lasers pumping is to match their radiation linewidth to the absorption line of the alkali atom. A typical Doppler broadened absorption line of pure alkali vapors is about 500 MHz which is many orders of magnitude less than a typical LDA's linewidth. There are two approaches for matching the LDA emission to the alkali atomic absorption that are explored now. First one is the use of a high pressure buffer gas to broaden the alkali absorption line to about 1 nm and to match it to the pump LDA linewidth. Another approach is narrowing of the LDA's linewidth to match it to the alkali vapor absorption line broadened by low pressure (about 1 atm) buffer gas. The required linewidth in this case is about 10 GHz. A combination of these two approaches, LDA line narrowing and buffer gas pressure increase, can also be considered.

Several methods utilizing different kinds of external cavities with wavelength sensitive elements have been developed [19–22] that significantly narrow the LDAs linewidth. In our experiments [23] we used holographic plane reflection grating and succeeded in narrowing the LDA linewidth to 11 GHz that well fits to the Cs absorption line broadened by a 1 atm buffer gas. Volume Bragg Gratings (VBGs) can also provide efficient enough LDA line narrowing (up to 7 GHz [22, 24]) though there are no published results on alkali lasers pumped by such narrow line LDAs.

4. Diode pumped alkali lasers

4.1. 10 W CW Cs laser

The first LDA pumped alkali laser was demonstrated by Page et al. in 2006 [25]. Using a pulsed VBG narrowed LDA with a linewidth 0.3 nm for pumping of Rb vapor they obtained about 1 W output peak power with slope

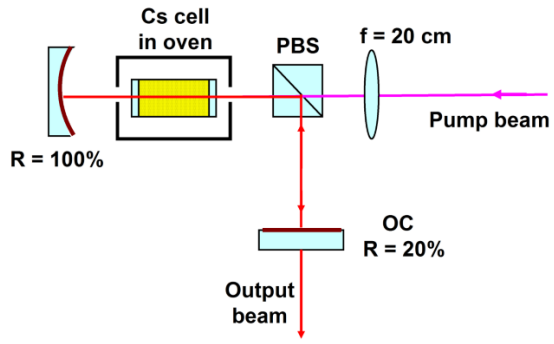

Figure 3. Schematic diagram of the diode pumped cesium laser.

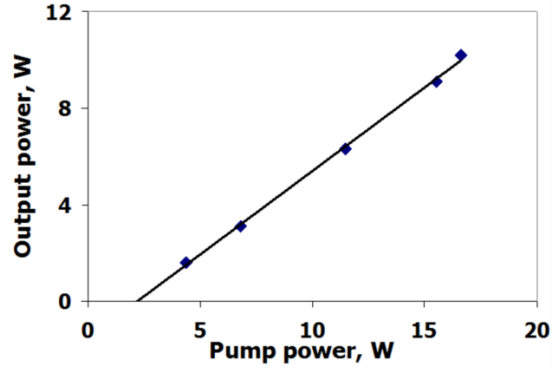

Figure 4. Output power of the Cs laser as a function of input pump power. The data shows 68% optical to optical slope efficiency, a 62% overall efficiency and an output power of 10 watts.

efficiency of 10% and total optical efficiency of 6%.

Recently, we demonstrated an LDA pumped continuous wave (CW) Cesium vapor laser with 10 W output and slope efficiency of 68% [8]. The laser cavity arrangement is presented in Fig. 3. The L-shape laser cavity consisted of a flat output coupler (20% reflectivity at 894 nm) and a high reflective 50 cm radius concave back mirror. The polarizing beam splitting cube was used to separate the pump and lasing beams, which had orthogonal polarizations. A 2 cm long cell with antireflection coated windows was filled with metallic cesium and 500 Torr ethane and placed in a temperature controlled oven. The LDA pump beam was focused into the center of the Cs cell by a lens with a focal length 20 cm.

The Cs laser output power dependence on the LDA pump power is shown in Fig. 4. An output power of 10 watts was obtained using 16 watts of incident laser diode array pump power, resulting in an overall optical to optical efficiency of 62% with a slope efficiency of 68%.

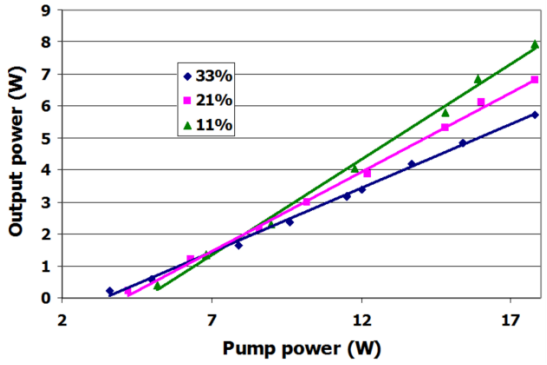

Figure 5. Output power of the Rb laser as a function of input pump power for different output couplers (33%, 21% and 11%). For the optimal output coupler of 11% the data shows 60% optical to optical slope efficiency, a 45% overall efficiency and an output power of 8 watts.

4.2. Diode pumped Rb laser

We implemented the technology, described above for the LDA pumped Cs vapor laser, to a Rb vapor laser In this experiment we employed the laser cavity design similar to presented in Fig. 3. We used a 2 cm long Rb cell with 600 Torr of ethane that was kept at the temperature of 103 - 106°C The cell was pumped by a narrowband LDA with operating wavelength of 780 nm. The experimental dependence of the Rb laser output power on the pump power was measured for the output couplers with reflectivities 33%, 21% and 11% (see Fig. 5). Corresponding measured values of the slope efficiencies for these output couplers are 40%, 49% and 60%. The maximum output power of 8 Watts was obtained with the 11% output coupler using 17.8 Watts of incident LDA pump power. The overall optical to optical efficiency was 45%.

5. Power scaling of alkali lasers

5.1. Rb laser with two LDA pump

Scaling of alkali lasers to higher powers requires using multiple diode lasers for pumping. We performed an experiment on pumping of a Rubidium laser by two continuous wave laser diode arrays with a total power of 37 Watts. The experimental apparatus used for this experiment is presented in Fig. 6. We used longitudinal pumping of the gain medium (Rb vapor) by the two pump beams, which entered the Rb cell from opposite sides, and were collinear with the lasing beam (and the laser cavity axis). To separate the pump beams from the lasing beam (which had orthogonal polarizations) we used two polariz-

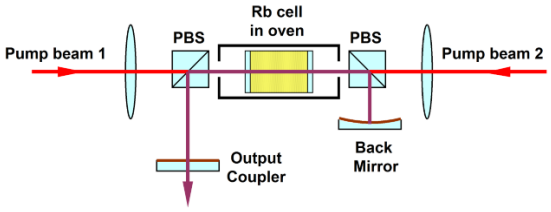

Figure 6. Schematic of the experimental setup. The polarizing beam splitters (PBS) are used so that the polarization of the laser is orthogonal to the polarization of two pump beams.

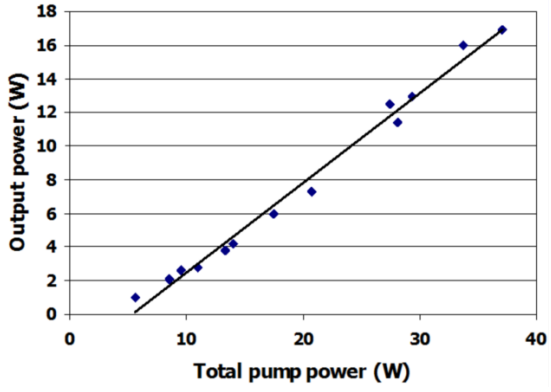

Figure 7. Output power of the Rb laser as a function of input pump power.

ing beam splitting cubes (PBS). The Π shape laser cavity had a length of 44 cm and was created by a high reflective 50 cm radius concave back mirror and a flat output coupler. The optimal reflectivity of the output coupler was determined experimentally to be 11%. A 2 cm long cell with antireflection coated windows was filled with metallic Rb and 600 Torr of ethane and placed in a temperature controlled oven. The LDAs pump beams were shaped by a Beam Transformation System (BTS-HOC, LIMO GmbH) and were focused into the center of the Rb cell by lenses with a focal length of 20 cm. An optimal value of the Rb cell temperature was determined experimentally to be in the range 103 – 106°C.

The experimental dependence of the Rb laser output power on the total pump power is presented in Fig. 7. This dependence was obtained by gradual changing of the output power of both pump sources from the threshold (about 5 Watts) to the maximum value (37 Watts). The maximum output power of 17 Watts was obtained with a slope efficiency of 53% and maximum overall optical to optical efficiency of 46%. The slope remained constant showing no saturation effects for these powers.

We also measured the Rb laser beam quality using a ModeMaster M^2 Beam Propagation Analyzer (Coherent). The propagation factors measured at a 0.5 m distance from the output coupler were $M_x^2 = 1.11$ and $M_y^2 = 1.10$ that are very close to a TEM_{00} Gaussian beam value. Good beam quality is important for applications requiring tight focusing or for second harmonic generation.

5.2. Cs laser with four LDA pump

For additional scaling we performed experiments on pumping a Cs vapor laser by four LDAs that allowed us to obtain up to 48 W of output power at 894 nm with an overall optical to optical efficiency of 49% and a slope efficiency of 52%.

The experimental setup is presented in Fig. 8. The Cs cell and oven designs were the same as in previous experiments. The Cs cell was filled with a mixture of Ethane (100 torr) and Helium (500 torr). The 40 cm long Cs laser cavity, which had a "Π" shape, was made by two mirrors: a 50 cm radius concave back mirror with near 100% reflection at 894 nm and a flat output coupler with 20% reflection at 894 nm. The cavity included two dichroic mirrors (DM), which had high reflections (98.8%) at 894 nm for s-polarization and high transmissions (88%) at 852 nm for unpolarized light, both at 45° angle of incidence. The dichroic mirrors were used for separating the lasing radiation (894 nm) from pumping radiation (852 nm), which entered into the Cs cell from both sides through these mirrors. Each of the four pump beams was focused into the center of the Cs cell by lenses (L) with a focal length of 20 cm. A pair of pump beams (#1 and #2, see Fig. 8), having orthogonal polarizations were combined in a polarization beam splitting cube (PBS) before entering the Cs cell from one side. The same was done for another pair of pump beams (#3 and #4), which entered the Cs cell from the opposite side. The pump beams were generated by narrowband LDAs with external cavities using techniques described earlier [23]. The maximum power of each pump source was about 25 W and their linewidth was less than 10 GHz.

We studied the characteristics of the Cs laser in both CW and pulsed operation. The pumping LDAs were powered in series by a pulsed current source with a pulse duration of 100 msec and a repetition rate of 1 Hz. We measured the output power and efficiency of the Cs laser for pump powers up to 100 W. The results are presented in Fig. 9. In pulsed mode the Cs laser output power grows linearly with the pump power and reaches 48 W at 98 W pump power that results in an overall optical efficiency of 49%. A linear fit to this data gives a slope efficiency of 52%. The efficiencies are slightly lower than the best result obtained for the diode pumped Cs laser [8], which can be due to mode mismatch and misalignment of the four pump beams and

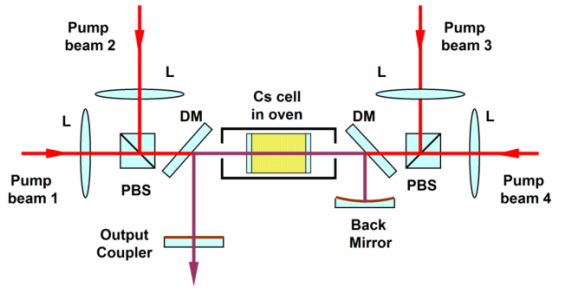

Figure 8. Schematic diagram of the Cs laser configuration. DM are dichroic mirrors, PBS are polarizing beam combiners and L are lenses.

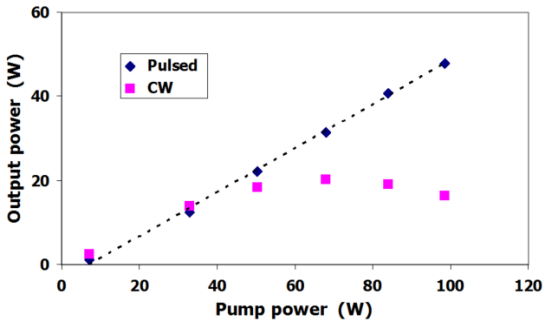

Figure 9. Cs laser output power for pulsed (diamonds) and CW (squares) operation depending on the pump power. The dashed line is a linear fit to the pulsed operation data showing a 52% slope efficiency.

the laser cavity mode, losses induced by dichroic mirrors and due not optimal transmission of the output coupler. In CW mode, the relation between the pump power and output power is no longer linear for high powers. The Cs laser output power is slightly higher for lower pumping powers (up to 30 W) in CW mode compared to pulsed operation, and then it rolls over and even drops at higher pump powers. Such behavior can be explained by thermal effects created by the heat released into the Cs vapor gain medium due to the energy defect ΔE between the $D1$ and $D2$ Cs lines (554 cm^{-1}). The quantum efficiency of the Cs laser is $\lambda_{D1} \,/\, \lambda_{D2} = 95.3\%$, which means that 4.7% of the pump power is released as heat into the gain medium. The resulting temperature rise can be estimated using a simple model. Consider the heat to be released from an imaginary cylinder of gas with dimensions defined by the laser beam size inside the Cs cell (2 cm in length and 0.08 cm in diameter). This heat consequently flows out to the cell walls (cell diameter is 2.5 cm). From the thermal conductivity of the buffer gas, the temperature difference between the cell center and the cell walls in a steady state regime can be found from the steady state heat equation [27]:

$$\frac{Q}{L} \ln\left(\frac{R}{r}\right) = 2\pi k \Delta T,$$

where Q is the amount of heat released per sec, $L = 2$ cm is the cell length, $R = 1.25$ cm and $r = 0.04$ cm are the radii of the cell and the heated cylinder of gas respectively, $k = 1.8\ \frac{\text{mW}}{\text{cm K}}$ is the heat conductivity of the buffer gas (Helium), and ΔT is the gas temperature difference between the cell center and the cell wall. For a pump power of 40 W, the heat released in the irradiated volume is about 2 W and that gives a temperature rise of $\Delta T \approx 300$ K. An improved model would include the Gaussian beam profile and heat convection.

This simple estimate for heat generation shows that there can be a significant temperature increase inside the irradiated volume of the gain medium even at pump power level of several tens of Watts. Such a temperature rise of the buffer gas inside the pump beam volume can create thermal lensing that changes the laser cavity configuration, destroys its stability and increases losses. Also contributing to the output power drop at higher temperatures is the possible increase in the rate of chemical reactions between Cs vapor and Ethane buffer gas. The products of these reactions (soot and cesium hydrate) create additional losses for the laser light because of absorption and light scattering which has been observed in previous works [8, 27–29].

5.3. Transversely pumped Cs laser

For the longitudinal pumping, this can be very complicated if more than four beams are to be combined. A transverse pumping, which is widely used in solid state lasers, has no such limitations. We performed experiments on transverse pumping of a Cs vapor laser by fifteen LDAs with total power of about 200 W.

The experimental setup is presented in Fig. 10. A 5 cm long and 3 mm inner diameter Cs vapor cell was filled with metallic cesium and the buffer gases ethane at 100 Torr and helium at 500 Torr pressures, measured at room temperature, before being sealed. The Cs cell was placed inside a cylindrical white diffuse reflector with inner diameter 10 mm, which had a 2 mm × 50 mm slit on its side, parallel to the cell axis. This slit was used to couple the pump beams inside the reflector volume. The ends of the reflector were covered by white diffuse reflecting caps with 2 mm holes for the laser output beam. The reflector with the Cs cell was assembled inside a temperature controlled oven. The 18 cm long Cs laser cavity was made by two mirrors: a 50 cm radius concave back mirror with near 100% reflection at 894 nm and a flat output coupler

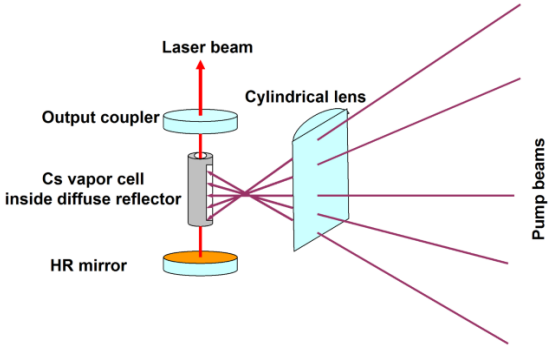

Figure 10. Schematic diagram of the transverse pumped Cs laser configuration.

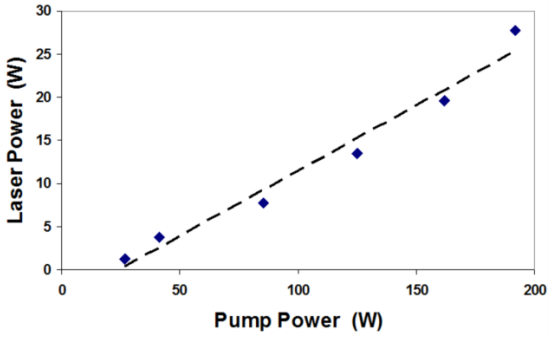

Figure 11. Cs laser output power dependence on pump power at an optimal temperature of 120°C.

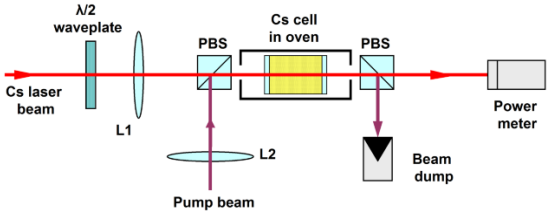

Figure 12. Cs amplifier - experimental apparatus.

with 20% reflection at 894 nm.

The gain medium was transversely pumped by fifteen pump beams, each of which was generated by a narrowband 852 nm LDA with external cavity, similar to described earlier [23]. The maximum power of each pump source was about 15 W and its linewidth was about 10 GHz. The LDA pump beams were individually collimated with a beam size of about 1 cm × 4 cm as measured at a 1 m distance from the diodes. The LDA pump lasers were arranged in 5 stacks with 3 LDAs in each stack. The beams from three lasers within a stack were made collinear to each other, separated vertically by about 1 cm making a "triple beam". The "triple beam" from each pump laser stack was incident on a large cylindrical lens, with a focal length of 20 cm, to be focused and coupled through the slit into the Cs vapor cell. The combined spot size of all 15 lasers was about 2mm by 5 cm at the entrance of the Cs cell. The angle of the incoming laser beams was less than 35 degrees.

We studied the characteristics of the transverse pumped Cs laser in pulsed operation. The pumping LDAs were powered in series by a pulsed current source with a pulse duration of 500 μs and a repetition rate of 20 Hz (duty factor is 1%). We intentionally didn't use higher repetition rate (or higher duty rate) or a CW pump to avoid thermal effects in cesium vapor, which are possible at high pump powers and observed previously (see above section). We measured the output power and efficiency of the Cs laser for pump powers up to 200 W at an optimal cell temperature of 120°C that was determined experimentally.

The Cs laser output power dependence on the pump power is presented in Fig. 11. The linear fit to this dependence (dashed line) gives a slope efficiency of 15%. A measured value of the maximum optical efficiency is 14%. The lower value of the slope efficiency compared to the longitudinally pumped Cs laser (68%, see [8]) can be due to a low pump coupling efficiency caused by the large difference between the cavity mode size inside the Cs cell (diameter is about 600 μm) and the inner volume of the diffuse reflector (diameter is 1 cm). As a result, the majority of the pump radiation does not illuminate the lasing volume and is not absorbed in it. To increase the pump efficiency (and, hence, the total laser efficiency), the laser cavity must be designed to have a mode volume close to the illuminated volume inside the reflector. This can be done, for example, by using an unstable laser cavity.

5.4. Diode pumped Cs vapor amplifier

Another way to increase an operating power of alkali lasers is to use optically pumped alkali amplifier or chain of amplifiers, like it is usually implemented in high power solid state laser systems. Chain of amplifiers has many advantages compared to single oscillator, because it allows simplifying a use of multiple pump sources and handling an excessive heat released into a gain medium.

The experimental setup is presented on Fig. 12. Cs vapor amplifier was assembled using a 2 cm long quartz cell filled with a metallic Cs and 500 torr of ethane buffer gas at room temperature. The cell was pumped by a narrowband LDA with external cavity, similar to described above, with a linewidth less than 10 GHz and operating at 852 nm. The pump beam was focused into the center of the cell through the Polarizing Beam Splitting cube (PBS) by the lens L2 with a focal length 20 cm. The input

signal beam with a wavelength 894 nm from a Cs laser, that had an orthogonal to the pump polarization, was also focused into the cell through the same PBS by a focusing lens L1 with a focal length 20 cm. For an efficient amplifier operation, the pump and input (amplified) beams must overlap each other and match in size along the whole cell. That is why the focal plane of the lens L1 was located behind the Cs cell to provide better matching of the input and pump beam sizes. The optimal position of the lens L1 was determined experimentally by maximizing of the output power while moving the lens along the input beam direction. The second PBS positioned behind the Cs cell separates amplified signal from the residual pump. The half wave plate installed in front of the lens L1 allows changing the power of the input beam by rotating it around the beam axis.

In these experiments we studied the operational parameters of the Cs amplifier, such as small signal amplification and gain for different pump levels and temperature (or density), dependence of the amplification on the input signal power. To determine an optimal vapor density (temperature) we performed measurements of the output power of the Cs amplifier at fixed low power input signal (10 mW) and fixed pump power (12 W) while changing the cell temperature. The measurements show that the amplification factor

$$A = \frac{P_{out}}{P_{in}}$$

grows with temperature and reaches its maximum value at the temperature 94°C. With further temperature increase, this dependence saturates and even rolls over. The reason for this is a too high vapor density and, thus, absorption, which do not allow pumping well through the whole cell length. The unpumped parts of the cell have a strong absorption for the signal beam, because it is a three-level gain medium.

If we consider that the gain coefficient for Cs vapor is constant along the gain medium (nonsaturated gain), its value G_{exp} can be estimated using the following formula:

$$P_{out} = P_{in} \exp\left(G_{exp} L\right),$$

where $L = 2$ cm is the Cs cell length. Correspondingly, the value of the gain coefficient is

$$G_{exp} = \frac{\ln A}{L}.$$

This value can also be calculated for the simple case of plane waves and highly pumped gain medium, when the pumped transition ($D2$) is saturated. In such approach the population N_1 of the ground state ($6S_{1/2}$) is twice lower

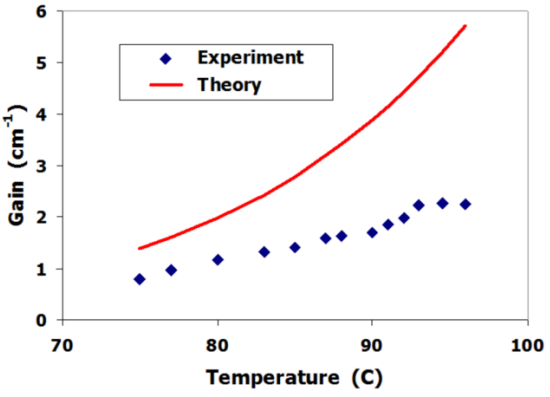

Figure 13. Cs amplifier experimental gain coefficient vs vapor temperature – comparison with theory.

than the population N_2 of the $6P_{3/2}$ state because of difference in degeneracy factors ($g_1 = 1$, $g_2 = 2$). The relation between the populations of the states $6P_{3/2}$ and $6P_{1/2}$ follows from Boltzmann equation

$$N_2 = \frac{g_2}{g_3} N_3 \exp\left(-\Delta E / kT\right),$$

where N_2 and N_3 are populations and g_2 and g_3=1 are the degeneracy factors of the $6P_{3/2}$ and $6P_{1/2}$ states correspondingly, ΔE is an energy difference between these two states, k is the Boltzmann constant and T is the vapor absolute temperature. Considering the three level pump scheme ($N_1 + N_2 + N_3 = N$ – vapor number density) we can calculate the population inversion on the lasing transition ($D1$): $\Delta N = N_3 - N_1$, and the gain coefficient $G_{calc} = \Delta N \sigma_1$, where σ_1 is a resonant cross section for D_1 line broadened by buffer gas. The value of σ_1 can be estimated as $\sigma_1 = \sigma_0$ (5 MHz / 10 GHz), where $\sigma_0 = 1.531 \times 10^{-9}$ cm^2 [9] is a resonant cross section for pure Cs vapor. The calculated values of the Cs gain coefficient G_{calc} as well as the values estimated from the experimental data G_{exp} are presented on Fig. 13. Experimental gain coefficient is about 1.5 – 3 times less than calculated and the difference grows with the cell temperature.

Such result was expected and it can be explained by a big difference between the real interacting beams and plane waves approach used for calculations. In addition, the beam size matching was also far from perfect and saturation effects can also not be neglected. But, in spite of all these discrepancies, the experimentally achieved gain in Cs vapors pumped by LDA appeared to be high enough for the practical applications. In our experiments with an 18 W pump LDA we had obtained small signal amplification factor up to 145 (see Fig. 14).

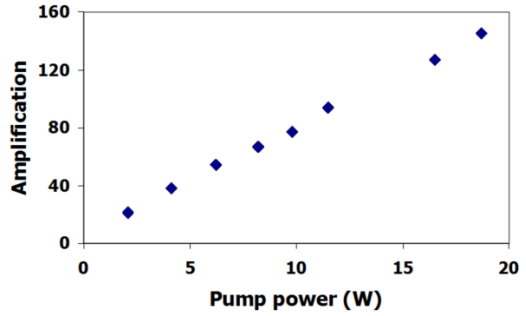

Figure 14. Cs amplifier small signal amplification factor vs pump power. Input signal is 10 mW, T = 94°C.

6. Tunable ring cavity Cs laser

Not only power requirements are important for such application as Spin Exchange Optical Pumping. A tunability of the laser source is also important for the fine tuning to the *D*1 resonance of alkali atoms. We have developed such a narrow-linewidth tunable source based on a ring cavity cesium vapor laser operating on the *D*1 transition ($6P_{1/2} \rightarrow 6S_{1/2}$) at a wavelength of 894 nm [29]. The measured linewidth of this laser was less than 3 MHz and tuning range of about 14 GHz.

A schematic of this laser is shown in Fig. 15. Pump light from a single mode Ti:Sapphire laser operating at 852 nm was focused into the center of a cesium cell using a 20 cm focal length lens (L). The 2 cm long cell contains metallic cesium and 600 torr of ethane buffer gas and was kept at a temperature of 87°C. The cell is positioned between two curved mirrors (M1 and M2) which together with flat mirrors M3 and M4 create a "bow tie" ring laser cavity. An optical diode (OD) positioned between two flat mirrors assures unidirectional lasing. A Fabry-Perot etalon (FP) with a free spectral range of 20.7 GHz and a finesse of 16 was used for providing single longitudinal mode operation and for course tuning of the lasing wavelength. Fine tuning was provided by a small translation of the M3 mirror by the piezo transducer (PT).

High resolution spectrum of the laser output obtained with a Fabry-Perot interferometer (see Fig. 16) demonstrates single longitudinal mode operation with a linewidth less than the interferometer instrument function, which is 3.3 MHz. The wavelength tuning range for this laser is limited by the width of the Cs lasing transition (*D*1) broadened by the ethane buffer gas. In our experiments the Cs absorption line was broadened by a 600 torr of ethane buffer gas to the value about 12 GHz. Tilting of the etalon allows to tune lasing wavelength on different resonator modes over the pressure broadened Cs line. Direct

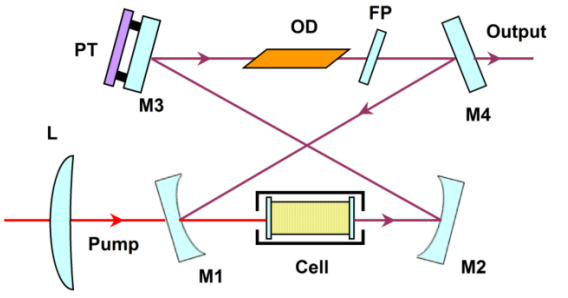

Figure 15. Ring cavity Cs laser setup: M1, M2, M3 and M4 – cavity mirrors, OD – optical diode, FP – Fabry-Perot etalon, PT – piezo transducer, Cell – Cs vapor cell in oven, L – focusing lens.

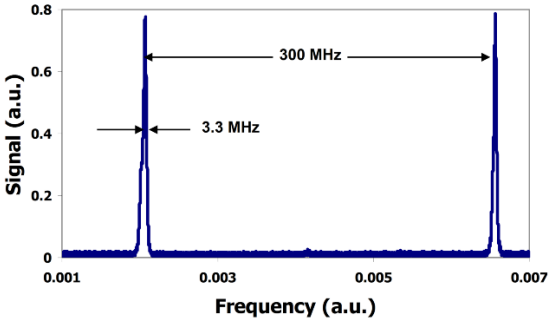

Figure 16. High resolution spectrum of the Cs laser output obtained with a Coherent interferometer (FSR 300 MHz) showing a single mode operation with a linewidth less than 3.3 MHz.

measurements of the radiation wavelength using Burleigh WA-1500 Wavemeter gave a tuning range about 14 GHz, from 894.586 nm to 894.625 nm measured in vacuum. The Cs *D*1 line wavelength in vacuum is 894.593 nm, which is included in the tuning range of this laser.

While we were not trying to optimize output power or slope efficiency in this experiment, we did take measurements of these data. The slope efficiency was 36% and the maximum output power was 80 mW. Using a diode laser pump, as it was done in experiments described above, will allow increasing the output power to a multi-watt level.

7. Conclusion

We presented a review of the main achievements in the field of alkali lasers development, demonstrating high potential of these lasers as a scalable source of high power laser radiation in the near infrared range. Remarkable proprieties of these lasers, like high efficiency, high beam quality, tunability, perfect match to *D*1 line of alkali atoms

makes them number one source for spin exchange optical pumping application. In addition, these lasers have simple design, high wall plug efficiency and can be produced commercially for many other applications.

Acknowledgements

We acknowledge support of the Air Force Office of Scientific Research, the Joint Technology Office for High Energy Lasers, and the National Science Foundation.

References

[1] J. R. MacFall et al., Radiology 200, 533 (1996)
[2] N. R. Newbury, A. S. Barton, G. D. Cates, W. Happer, H. Middleton, Phys. Rev. A 48, 4411 (1993)
[3] Th. G. Walker, W. Happer, Rev. Mod. Phys. 69, 629 (1997)
[4] W. F. Krupke, R. J. Beach, V. K. Kanz, S. A. Payne, Opt. Lett. 28, 2336 (2003)
[5] T. Ehrenreich, B. Zhdanov, T. Takekoshi, S. P. Phipps, R. J. Knize, Electronics Lett. 41, 47 (2005)
[6] T. A. Perschbacher, D. A. Hostutler, T. M. Shay, Proc. SPIE 6346, 63467 (2007)
[7] B. V. Zhdanov, T. Ehrenreich, R. J. Knize, Opt. Commun. 260, 696 (2006)
[8] B. V. Zhdanov, R. J. Knize, Opt. Lett. 32, 2167 (2007)
[9] B. V. Zhdanov, J. Sell, R. J. Knize, Electron. Lett., 44, 582 (2008)
[10] J. Zweiback, B. Krupke, A. Komashko, Proc. SPIE 6874, 68740G1-7 (2008)
[11] B. V. Zhdanov, A. Stooke, G. Boyadjian, A. Voci, R.J. Knize, Opt. Lett. 33, 414 (2008)
[12] A. L. Schawlow, C. H. Townes, Phys. Rev. 112, 1940 (1958)
[13] T. H. Maiman, Nature 187, 493 (1960)
[14] S. Jacobs, G. Gould, P. Rabinowitz, Phys. Rev. Lett. 7, 415 (1961)
[15] P. Rabinovitz, S. Jacobs, G. Gould, Appl. Optics 1, 513 (1962)
[16] Z. Konefal, Opt. Comm. 164, 95 (1999)
[17] R. J. Beach, W. F. Krupke, V. K. Kanz, S. A. Payne, J. Opt. Soc. Am. B 21, 2151 (2004)
[18] T. Ehrenreich, B. Zhdanov, T. Takekoshi, S. P. Phipps, R. J. Knize, Electron. Lett. 41, 47 (2005)
[19] E. Babcock, B. Chann, I. Nelson, T. Walker, Appl. Opt. 44, 3098 (2005)
[20] C. Talbot et al., Appl. Opt. 44, 6264 (2005)
[21] Y. Zheng, H. Kan, Opt. Lett. 30, 2424 (2005)
[22] L. S. Meng et al., Opt. Express 14, 10469 (2006)
[23] B. V. Zhdanov, T. Ehrenreich, R. J. Knize, Electron. Lett. 43, 221 (2007)
[24] A. Gourevitch, G. Venus, V. Smirnov, L. Glebov, Opt. Lett. 32, 2611 (2007)
[25] R. Page, R. Beach, V. Kanz, W. Krupke, Opt. Lett. 31, 353 (2006)
[26] H. S. Carslaw, J. C. Jaeger, Conduction of heat in solids, 2nd edition (Oxford science publications, Clarendon Press, Oxford, 1985)
[27] A. Tam, G. Moe, W. Happer, Phys. Rev. Lett. 35, 1630 (1975)
[28] B. Zhdanov et al., Opt. Commun. 270, 353 (2007)
[29] B. V. Zhdanov et al., Opt. Commun. 280, 161 (2007)